Earthquake Engineering, Tenth World Conference © 1992 Balkema, Rotterdam. ISBN 90 5410 060 5

Spatial characteristics of soil liquefaction and induced behavior of underground pipelines

Hideo Matsumoto & Ken-ichi Tokida
Public Works Research Institute, Tsukuba, Japan

ABSTRACT: Spatial occurrence characteristics of soil liquefaction and their effects on the dynamic behavior of underground pipelines are investigated based on shaking table tests with the use of a square container of 8 m long, 1 m wide and 1 m high where sandy ground models and pipe models are prepared. Experimental results are given which show the effects of horizontal spread of liquefiable ground, and the relationship between the degree of soil liquefaction, the spatial irregularity of ground condition and the induced behavior of underground pipes.

1 INTRODUCTION

Iwasaki, Tatsuoka, Tokida and Yasuda (1978) proposed a simplified procedure to estimate the liquefaction potential of loose and saturated sandy layers with the use of a liquefaction resistance factor F_L defined by the equation (1).

$$F_L = R / L \tag{1}$$

where F_L is the liquefaction resistance factor, R is the resistance of soil elements to dynamic loads and L is the dynamic load applied to the soil elements. The simplified procedure to estimate R and L from an engineering view point was applied in the seismic design specification for highway bridges established in 1980 and revised in 1990 by the Japan Road Association (1980, 1990), and was also applied in the seismic design guidelines for common utility ducts established by the Japan Road Association (1986) with the use of the following equations.

$$R = R_1 + R_2 + R_3 \tag{2}$$

$$R_1 = 0.0882\sqrt{N/(\sigma_v'+0.7)} \tag{3}$$

$$R_2 = \begin{cases} 0.19 & (0.02\text{mm} \leq D_{50} \leq 0.05\text{mm}) \\ 0.225\log_{10}(0.35/D_{50}) & (0.05\text{mm} < D_{50} \leq 0.6\text{ mm}) \\ -0.05 & (0.6\text{ mm} < D50 \leq 2.0\text{ mm}) \end{cases} \tag{4}$$

$$R_3 = \begin{cases} 0.0 & (0\,\% \leq F_c \leq 40\,\%) \\ 0.004 \cdot F_c - 0.16 & (40\,\% < F_c \leq 100\,\%) \end{cases} \tag{5}$$

$$L = r_d \cdot k_e \cdot (\sigma_v/\sigma_v') \tag{6}$$

$$r_d = 1.0 - 0.015 \cdot z \tag{7}$$

$$k_e = C_Z \cdot C_G \cdot C_I \cdot k_{SO} \tag{8}$$

where R_1 is the resistance based on relative density, R_2 is the resistance based on D_{50}-values, R_3 is the resistance based on fine contents, N is the blow count by standard penetration test, D_{50} is the mean grain size (mm), F_c is the fines content (%), z is the depth from the actual ground surface (m), k_e is the seismic coefficient for evaluating liquefaction, C_Z is the seismic zone factor(Zone-A:1.0, Zone-B:0.85, Zone-C:0.7), C_G is the ground condition factor(Ground Group I :0.8, Ground Group II :1.0, Ground Group III :1.2), C_I is the importance factor(1st Class:1.0, 2nd Class:0.8), k_{SO} is the standard seismic coefficient (= 0.15), σ_v is the total overburden (kgf/cm^2) and σ_v' is the effective overburden pressure under static conditions (kgf/cm^2).

The factor of F_L can be obtained at any depth of subsurface ground and layers with liquefaction resistance factor F_L smaller than 1.0 are judged to liquefy during earthquakes. In this procedure, the sandy ground of interest is assumed to spread uniformly in a horizontal direction and a liquefaction potential is estimated at a certain point of ground surface.

However, because such a structure as an underground pipeline spreads widely and the subsurface ground condition is not uniform horizontally in practice, the spatial ground condition, in other words, the effect of an irregularity of ground should be investigated much more for establishing a reasonable seismic design method of underground structures such as pipelines and ducts.

Typical relations between spatial liquefiable ground conditions and

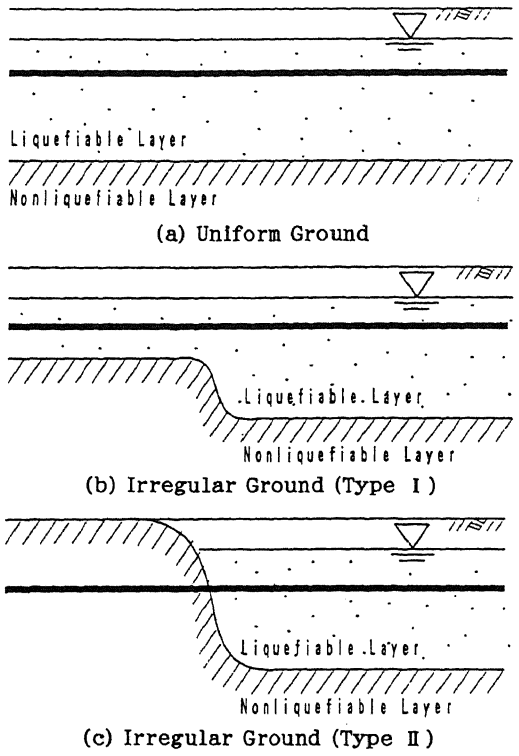

Figure 1. Typical relations between spatial liquefiable ground conditions and underground structures (pipes/ducts).

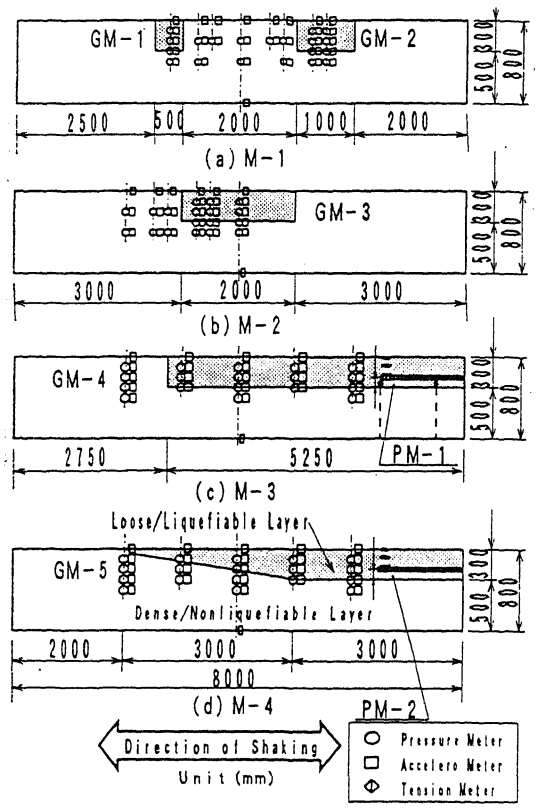

Figure 2. Ground models and measurements

underground structures such as pipes and ducts can be classified into three types as shown in Figure 1. In the case of a uniform ground as shown in Figure 1 (a), the underground structure is deformed by the uplift force induced by a soil liquefaction.

On the other hand, for an irregular ground as shown in Figures 1 (b) and (c), not only an uplift force but also a section force is induced by the difference of the soil liquefaction potential or uplift force through the irregular ground work on the underground structure.

This paper describes spatial occurrence characteristics of soil liquefaction and their effects on the dynamic behavior of underground pipelines investigated based on shaking table tests. Experimental results indicate the importance of considering the effects of a horizontal spread of liquefiable ground and show the relationship between the degree of soil liquefaction, the spatial irregularity of the ground condition and the induced behavior of underground pipes.

Table 1. Conditions of ground models

Model No.		GM-1	GM-2	GM-3	GM-4	GM-5
Liquefiable Layer	Thickness (mm)	300		300	300	300
	Length (mm)	500	1000	2000	5250	3000~6000
	Void Ratio e	0.703		0.728	0.861	0.843
	Relative Density Dr(%)	70		62	25	34
	Shear Wave Velocity Vs (m/s)	46		36	43	44
Nonliquefiable Layer	Void Ratio e	0.565		0.670	0.652	0.611
	Relative Density Dr(%)	105		76	82	92
	Shear Wave Velocity Vs (m/s)	110		112	65	78

2 METHOD OF EXPERIMENTS

2.1 Ground model and pipe model

Five liquefiable ground models (MG-1~5) are set up in a square container placed on a shaking table. The conditions of the ground models are shown in Figure 2 and Table 1. The container is 8 m long, 1 m wide and 1 m high. Six transparent glass windows (each 0.8 m wide and 1.0 m high) are installed at the one side of the square container. The models consist of two layers: a loose liquefiable layer and a lowermost stiff nonliquefiable layer. The ground water level is set equal to the ground model

Table 2. Characteristics of ground model materials

Specific Gravity of Soil Particle G_s	2.617
Maximum Void Ratio e_{max}	0.587
Minimum Void Ratio e_{min}	0.977
Mean Grain Size D_{50} (mm)	0.22
Coefficient of Uniformity Uc	2.00

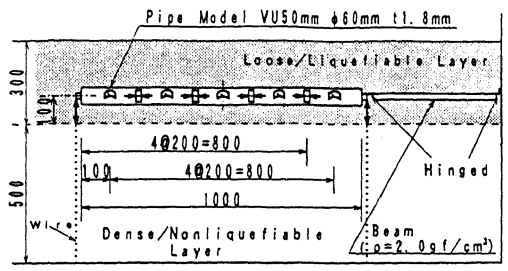

Pipe Model 1 (PM-1)

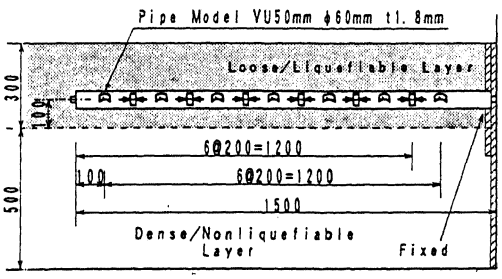

Pipe Model 2 (PM-2)

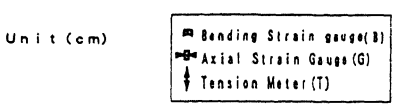

Figure 3. Conditions of pipe models

surface. As shown in Table 1, the thickness of a liquefiable layer is 300 mm and the length of it ranged from 500 mm (GM-1) to 6,000 mm (GM-5). The materials used for both a liquefiable layer and a nonliquefiable layer are Toyoura Sand which is very clean sand as shown in Table 2.

As for preparation of the models, the lowermost nonliquefiable layer is first compacted enough in the container not to liquefy during excitation, a certain amount of water is poured, and then the liquefiable layer is prepared by means of the underwater drop method.

In the cases of Ground Model-4 and Ground Model-5, two types of pipes were laid in the liquefiable layers as shown in Figure 3. The

Table 3. Input conditions of shaking table

Model No.	Shaking Step No.	Maximum Acceleration at Table α max(gal)	Input Motion
GM-1	1	31	Sinusoidal
GM-2	2	49	5Hz
	3	65	8sec
	4	85	(40cycles)
	5	102	
	6	121	
	7	139	
	8	158	
	9	177	
GM-3	1	84	
	2	102	
	3	121	
	4	140	
	5	177	
	6	216	
GM-4	1	80	
	2	98	
	3	115	
	4	134	
	5	170	
	6	207	
GM-5	1	82	
	2	99	
	3	117	
	4	135	
	5	172	
	6	210	
	7	268	

pipe model (P-1) made of vinyl chloride for Model-4 was 1.0 meter long, and the diameter and thickness were 60 millimeter and 1.8 millimeter, respectively. One of the pipe ends was free and the other one was hinged with a rigid beam hinged at the wall of the shaking table. The pipe (P-2) made of vinyl chloride for Model-5 was 1.5 meter long, and the diameter and thickness were 60 millimeter and 1.8 millimeter, respectively. One of the pipe ends was free and the other one was fixed at the wall of the shaking table.

2.2 Measurements

As shown in Figure 1, accelerometers, pore water pressure meters, strain gage meters and displacement meters are installed in or on both liquefied and nonliquefied layers to measure the time history of acceleration and pore water pressure of layers during excitation. Strain gages to measure the bending strains and axial strains of a pipe model induced by soil liquefaction were put on the upper and lower portions of a pipe model and the two sides of it. Furthermore, two tension meters connected with wires between the pipe ends and the bottom of the shaking table were set to measure the time history of the uplift force on the pipe. The acceleration at the surface of a shaking table is also measured as an input motion for a ground model.

2.3 Input Condition

In each test, a constant sinusoidal acceleration with a frequency of 5 Hz is employed to drive a shaking table for 8 seconds (40 cycles), and several levels of maximum acceleration (31 ~ 268 gals) are

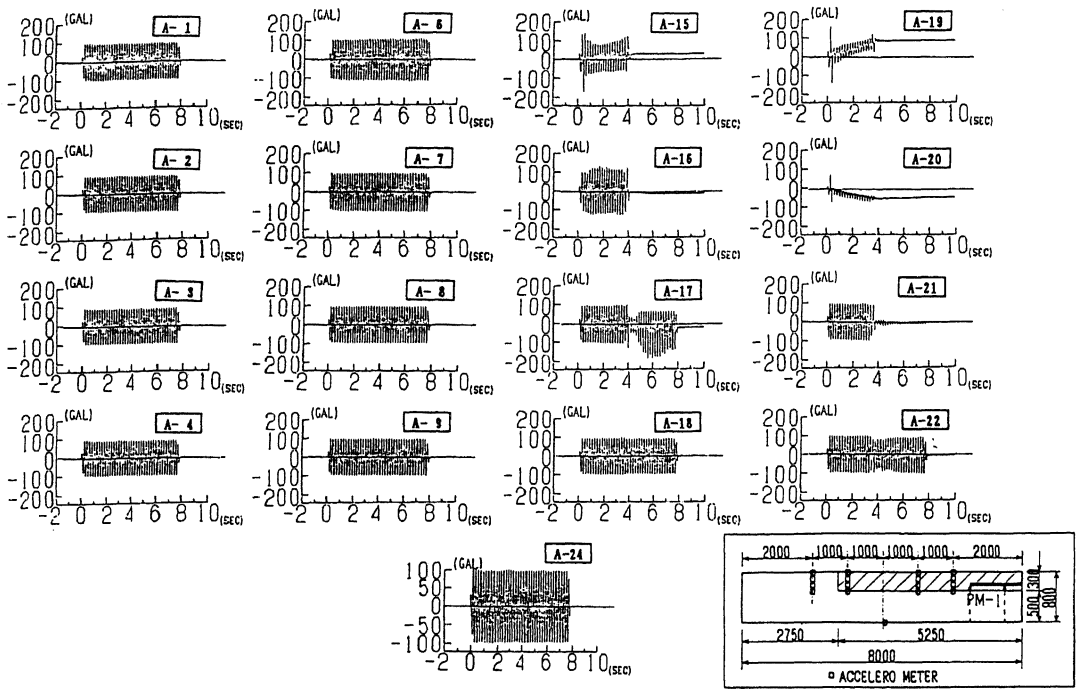

(a) Acceleration in the ground model

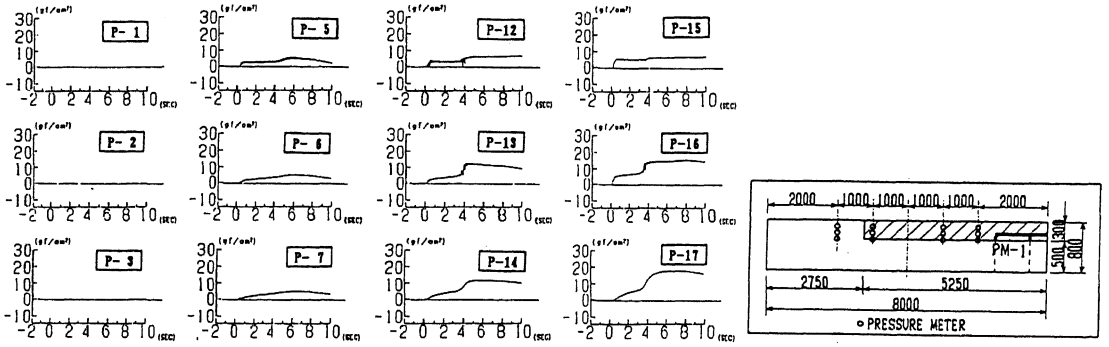

(b) Excess pore water pressure in the ground model

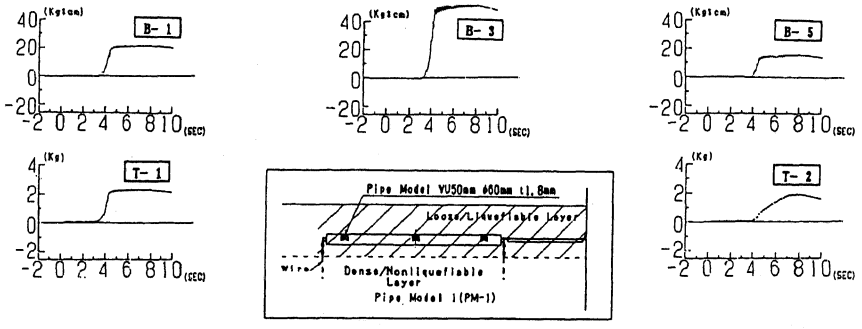

(c) Bending moment in the pipe model and uplift force at the end of pipe model

Figure 4. Time history of dynamic behavior of ground model and pipe model (Ground Model-4, Step-2: α_{Bmax}=98 gal)

applied stepwise to a shaking table as input motion. The measured maximum acceleration of the shaking table are summarized as shown in Table 3 for all test steps of each model case.

3 SPATIAL GROUND MOTION INDUCED BY SOIL LIQUEFACTION

Figures 4(a) and 4(b) show a typical result of time histories of input ground acceleration and excess pore water pressure, respectively, at the Step-2 in the case of Ground Model-4 (GM-4). Based on these Figures, the following can be deduced:

1)The ground acceleration in the nonliquefiable ground was almost same as the input motion (see Points A-1～A-4) and excess pore water pressure (Δu) did not occur (see Points P-1～A-3).

2)The acceleration in the liquefiable ground close to the boundary between the liquefiable ground and the nonliquefiable one was almost same as the one in the nonliquefiable ground (see Points A-6～A-9). However, the excess pore water pressure increased a little (see Points A-5～A-7).

3)In the middle of liquefiable ground, the ground seemed to be liquefied perfectly at about 3.5 to 4 seconds of elapsed time after the start of shaking, because the ground acceleration decreased to zero. Furthermore, it can be noticed that the ground liquefied perfectly at the section of the Point A-19 (same location as P-15). This was deeper than that at the section of the Point A-15 (same location as P-12) (see Points A-15, 16, 19～21/P-12, 15, 16).

Figure 5 shows the distribution of maximum excess pore water pressure ratio for all ground models (GM-1～5) and for the same input motion of about 100 gals. Based on this figure, the following can be noted:

1)The liquefiable ground was not almost liquefied in the cases of Ground Models 1, 2 and 3. The maximum excess pore water pressure ratio was about 0.1 in each case.

2)In the case of Ground Model-4, the liquefiable ground was liquefied perfectly.

3)In the case of Ground Model-5, the liquefiable ground was partially liquefied in the measured area. The maximum excess pore water pressure ratio was about 0.6.

Table 4 summarizes the relation between the input motion, the length of liquefiable ground and a maximum excess pore water pressure ratio measured during each shaking. Based on this table, it can be noted that the liquefiable ground becomes more liquefiable

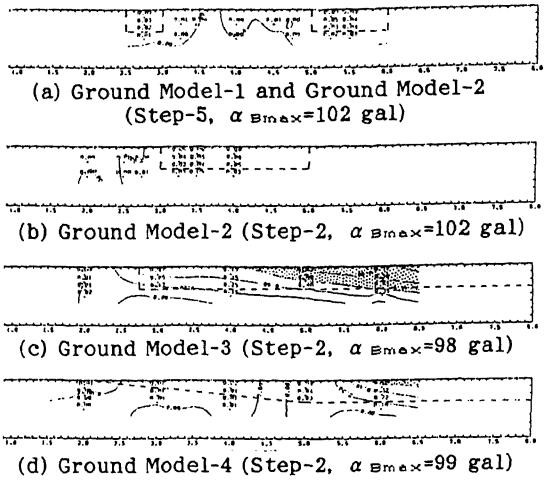

(a) Ground Model-1 and Ground Model-2 (Step-5, α_{Bmax}=102 gal)

(b) Ground Model-2 (Step-2, α_{Bmax}=102 gal)

(c) Ground Model-3 (Step-2, α_{Bmax}=98 gal)

(d) Ground Model-4 (Step-2, α_{Bmax}=99 gal)

Figure 5. Distribution of excess pore water pressure in the ground model according to spread of liquefiable ground.

Table 4. Magnitude of input motion and ground surface acceleration at nonliquefiable ground according to spread of liquefiable ground.

Model No.		GM-1	GM-2	GM-3	GM-5	GM-4
Length of Liquefiable Layer (m)		0.5	1.0	2.0	3.0 ↓ 5.0	5.25
Maximum Acceleration at Table α max(gal)	80	0.0	0.0	0.0	0.0	0.7
	100	0.1	0.1	0.1	0.6	1.0
	120	0.1	0.1	1.0	1.0	1.0
	140	0.2	1.0	1.0	---	---
	160	1.0	0.8	---	1.0	1.0
	180	0.8	0.6	1.0	1.0	0.9
	220	---	---	1.0	1.0	0.9
	280	---	---	---	1.0	---

▒ : Power Water Pressure Ratio ≥ 0.6

in proportion to the increase of the horizontal spread of liquefiable ground.

4 DYNAMIC BEHAVIOR OF PIPES INDUCED BY SOIL LIQUEFACTION

The pipe model was forced to lift up according to the progress of soil liquefaction. Figure 4(c) shows the time history of the bending moment in the pipe and the uplift force at the end of pipe model. The left end of the pipe model is located close to the pore water pressure meter P-16 (see Figure 2). Comparing Figure 4(c) with Figure 4(b), it can be found that the bending moment and the uplift force begin to increase rapidly according to the rapid increase of the excess pore water pressure. In this case, at about 3.5 seconds of elapsed time

after the start of shaking, the bending moment and uplift force become constant at about 4 seconds of elapsed time when the ground surrounding the pipe model is liquefied perfectly.

Figure 6 shows the relations between the bending moment in the pipe model (Point B3), the up-lift force at the end of the pipe model (Point T-1) and the excess pore water pressure (Point P-16) in the surrounding liquefiable layer. From this figure, it can be seen that in the case of Step-1, the liquefiable layer was not liquefied to such an extent to produce a substantial increase in the bending moment and up-lift force. On the other hand, in the case of Step-2, both bending moment and up-lift force increased according to the increase of excess pore water pressure, in other words, to the progress of soil liquefaction.

Based on Figures 4 and 6, it can be noted that the uplift deformation of a pipe model begins to increase rapidly when the excess pore water pressure ratio ($\Delta u / \sigma_v'$) increases more than about 0.6 ~0.8.

The maximum tension load measured by tension meters (T-1 and T-2) at the left-end and right-end of the pipe model were 2.5 kgf and 2.0 kgf, respectively. On the other hand, because the weight of the pipe model (P-1) was 0.8 kgf, the up-lift force acting on the pipe could be calculated to be 5.3 kgf (= 4.5 kgf + 0.8 kgf). When the liquefiable layer was liquefied perfectly, the unit weight of liquefied soils could be calculated to be 1.87 gf/cm^3 (= 5.3 kgf/2,827 cm^3), because the volume of the pipe model was 2,827 cm^3 (ϕ 60 mm × 1 m).

5 CONCLUSIONS

The main results of this study can be described as follows:

1)The liquefiable model ground in the shaking table tests becomes more liquefiable in proportion to the increase in the horizontal spread of liquefiable layers for the same input motion. The reason of this is the confinement by the nonliquefiable ground neighboring the liquefiable ground.

2)Therefore, it is necessary to consider the spatial irregularity of ground in situ to estimate a soil liquefaction potential such as F_L-value defined by the equation (1). In practice, the ground irregularity should be considered to estimate the dynamic load such as L defined by the equation (6). Tokida and Tamura (1992) have investigated the effects of the ground irregularity on the amplification of ground motion.

3)The ground acceleration increases in proportion to the increase of excess pore water pressure and decreases to almost zero rapidly when the excess pore water pressure

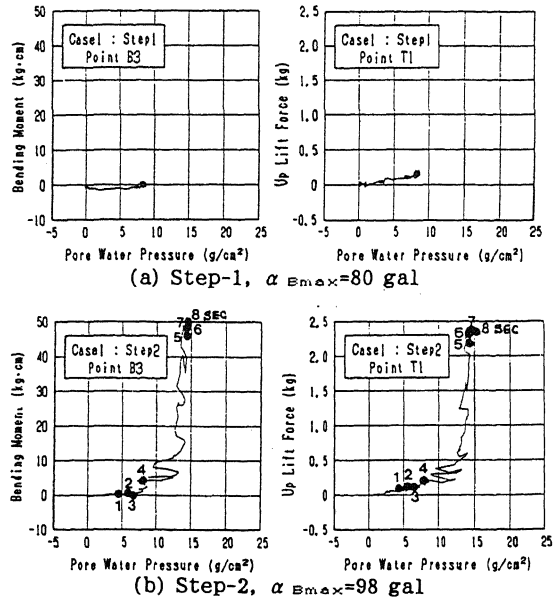

(a) Step-1, α_{Bmax}=80 gal

(b) Step-2, α_{Bmax}=98 gal

Figure 6. Relation between bending moment occurred in the pipe model, uplift force working at the end of pipe model and excess pore water pressure (Ground Model-4).

approaches the effective overburden pressure. This indicates that softened ground by soil liquefaction amplifies the ground motion just before perfect liquefaction.

4)The uplift deformation of a pipe model begins to increase rapidly when the excess pore water pressure ratio becomes more than about 0.6 ~ 0.8. In other words, pipelines are not deformed severely by the uplift force when the soil liquefaction potential is low. Similar behavior was found for the lateral ground flow induced by soil liquefaction of inclined ground as reported by Sasaki, Tokida, Matsumoto and Saya (1991).

Further investigation should be conducted on the dynamic behavior of pipelines buried at the boundary between a liquefiable ground and a nonliquefiable one and on the reasonable seismic design methods of pipelines in the future.

ACKNOWLEDGEMENTS

The authors wish to express their sincere gratitude to Professor Timothy B. D'Orazio of San Francisco State University who visited the Ground Vibration Division of Public Works Research Institute (PWRI) as an invited researcher by the STA (Science and Technology Agency) Fellowship and Mr. Takuo Azuma of PWRI for their assistance to present this report.

REFERENCES

Iwasaki, T., Tatsuoka, F., Tokida, K. and Yasuda, S. 1978. A practical methods for assessing liquefaction potential based on case studies at various sites in Japan. Proceedings of 5th Japan Symposium on Earthquake Engineering, Tokyo, Japan: 641-648 (in Japanese).

Japan Road Association 1980, 1990. Part V Seismic Design of Design Specifications for Highway Bridges (in Japanese).

Japan Road Association 1986. Design Guidelines for Common Utility Ducts (Proposal) (in Japanese).

Tokida, K. 1992. Assessment of liquefaction potential and its treatment for design and construction of civil engineering structures. Technical Memorandum of Public Works Research Institute, Vol. 3091.

Tokida, K. and Tamura, K. 1992. Effects of geological and topographical irregularities on ground motion characteristics, 10th World Conference of Earthquake Engineering, Madrid, Spain.

Sasaki, Y., Tokida, K., Matsumoto, H. and Saya, S. (1991). Experimental study on lateral ground flow of ground due to soil liquefaction. 2nd International Conference on Recent Advances in Geotechnical Earthquake Engineering and Soil Dynamics, St. Louis, Missouri, USA.